Final Draft
Manuscript available at: https://doi.org/10.1061/(ASCE)BE.1943-5592.0000871
Full citation: Gerbo, EJ, Casias, CM, Thrall, AP, and Zoli, TP (2016) "New Bridge Forms Composed of Modular Bridge Panels." Journal of Bridge Engineering, 21(4), 04015084

New Bridge Forms Composed of Modular Bridge Panels

Evan J. Gerbo, S.M.ASCE[1]; Casey M. Casias, S.M.ASCE[2];
Ashley P. Thrall, A.M.ASCE [3]; Theodore P. Zoli, P.E., M.ASCE [4]

ABSTRACT

Panelized bridge systems (e.g., Bailey, Mabey-Johnson, Acrow) are intended for girder-type bridges and have been implemented for military, civilian, and disaster relief applications. Design challenges, however, include material efficiency (span squared per number of panels), lateral bracing, and achieving longer spans. These challenges are addressed by investigating the promise of implementing panels in new configurations with longer spans and evaluating bracing strategies. Three new forms (Pratt truss, bowstring truss, and network tied arch) composed of standard length panels, with shapes determined based on geometric considerations and structural performance (resistance to buckling), are presented. A parametric study evaluates lateral bracing strategies for girder- and column-like configurations. The promise of the new forms, also incorporating the developed bracing strategy, is demonstrated through finite element analyses. Following this investigation using a standard length panel, an optimization procedure for minimum self-weight and maximum structural performance is developed to determine an optimized panel length and form. This paper addresses the design challenges of efficiency, bracing, and span length for panelized bridge systems and indicates future areas for improvement through optimization.

CE Database subject headings: Bridges; Modular structures; Prefabrication; Bracing

INTRODUCTION

Modular panelized bridge systems are appealing since they are comprised of prefabricated

[1]Graduate Student, Kinetic Structures Laboratory, Department of Civil and Environmental Engineering and Earth Sciences, University of Notre Dame, Notre Dame, IN 46556. E-mail: egerbo@nd.edu

[2]Graduate Student, Kinetic Structures Laboratory, Department of Civil and Environmental Engineering and Earth Sciences, University of Notre Dame, Notre Dame, IN 46556. E-mail: ccasias@nd.edu

[3]Myron and Rosemary Noble Assistant Professor of Structural Engineering, Kinetic Structures Laboratory, Department of Civil and Environmental Engineering and Earth Sciences, University of Notre Dame, Notre Dame, IN 46556. (corresponding author) E-mail: athrall@nd.edu

[4]National Bridge Chief Engineer, HNTB Corporation, New York, NY 10001. E-mail: tzoli@hntb.com

components, can be rapidly erected in the field, and offer significant versatility. Standard, commercially available systems - including the Bailey, Mabey-Johnson, and Acrow systems (Figure 1) - consist of 3.05 m (10 ft) long panels and are typically arranged longitudinally to form a girder-type bridge. Additional panels can be combined transversely and/or vertically to increase the width, span, or load carrying capacity of the bridge. They have been widely used for military, civilian, and disaster relief applications since World War II (Joiner, 2001; Russell and Thrall, 2013).

Design challenges for these systems which this paper aims to address include (1) efficient use of material (quantified as span squared per number of panels), (2) lateral bracing, and (3) achieving longer spans. To reach long spans [on the order of 61.0 m to 91.4 m (200 to 300 ft)], these systems must take a double-triple (i.e., two panels transversely and three panels vertically for each plane of the bridge; shown for the Bailey system in Figure 2) or triple-triple configuration (i.e., three panels transversely, three panels vertically). These stacked configurations, however, result in material being placed where it is not needed. More specifically, bending is resisted primarily by the upper chord of the highest panel and the bottom chord of the lowest panel, while the remaining chords approach the neutral axis and contribute little to bending capacity. Furthermore, stacking does not vary with the moment demand along the length of the span. Similarly, the same shear capacity is provided throughout the span despite varying demand. This results in material inefficiency as a large number of panels are required to achieve desired spans. Overall, the span of the girder-type configurations is limited by buckling of the upper chord of the highest panel. Lateral bracing is required to mitigate this behavior. However, lateral bracing is expensive and time-consuming to install. Geometric challenges also result in a stacked through-type bridge. When stacked three high vertically in a through-type bridge, lateral bracing can be implemented on top of the highest panel as shown in Figure 2. If stacked only one or two panels high, this bracing is not practical as it would interfere with traffic flow. As demonstrated by the implementation of triple-triple configurations, longer spans are desired. Due to the flexural behavior of the conventional girder-type configuration, barriers to achieving longer spans include 1) material inefficiency that results from stacking and 2) lateral bracing strategies which mitigate buckling of the upper chord.

To achieve longer spans with enhanced material efficiency, this paper investigates truss and arch forms which primarily carry load axially as opposed to the primarily flexural behavior of the conventional girder-type configuration. More specifically, this paper investigates the potential for implementing panels in 1) Pratt truss, 2) bowstring truss, and 3) network tied arch forms. These new forms, comprised of standard 3.05 m (10 ft) long panels (i.e., the length of each of the panels in the Bailey, Mabey Johnson and Acrow systems, Figure 1), are investigated for a span exceeding 91.4 m (300 ft). The geometry of the forms are determined based on geometric considerations and structural performance (quantified by a metric related to buckling resistance). Integral to investigating these forms is an evaluation of lateral bracing. Toward this end, a parametric study is performed on a girder-like and a column-like configuration of panels which investigates the effect of spacing between planes of panels and bracing members on buckling behavior. With a bracing scheme determined, three-dimensional finite element analyses are performed to show the promise of these forms. The material efficiency of these forms are compared to a conventional girder-type configuration. Following this analysis using the standard 3.05 m (10 ft) long panels, the solution space is widened to investigate alternative panel lengths. A multi-objective optimization procedure for minimum self-weight and maximum structural performance is developed to determine an optimized panel length and form for panelized bridge systems. This procedure is demonstrated for the bowstring truss form. This paper ultimately addresses the design challenges of material efficiency, lateral bracing, and achieving longer spans for panelized bridge systems and indicates future areas for improvement of panelized systems through structural optimization.

BACKGROUND

The Bailey Bridge, designed following World War I, was the first panelized system that featured rapid erection through the implementation of pin connections between standard, prefabricated panels and versatility in its stackability both transversely and vertically (Joiner, 2001). The Bailey panel is comprised of top and bottom chords, vertical, and diagonal components that are welded together. Panels are joined together longitudinally by pins connecting male and female lugs at the top and bottom chords of adjacent panels. Floor beams, called transoms, are clipped to the lower chord of panels and support stringers and ultimately the deck (Department of the Army, 1986). It can serve as a simple-span, through, girder-type bridge (Figure 3A), with additional capacity by adding panels transversely and/or vertically (Figure 3B) as well as by adding a cable reinforcement set (Figure 3C) (Thierry, 1946; Department of the Army, 1986). They can be adapted to be a two-lane, through-type (i.e., combining multiple single-lane, through-type spans, Figure 3D) or a two-lane deck type (i.e., applying a deck on top of panels to facilitate wider roadways and overhangs, Figure 3E) (Department of the Army, 1986). When supported by barges, a Bailey Bridge can also serve as a floating bridge (Figure 3F). The utility and versatility of the Bailey Bridge has been demonstrated since World War II, when it was the principal tactical fixed bridge of the Allied Forces and the British Army's standard floating bridge (Thierry, 1946). The U.S. Army currently uses the Standard US Army M2 panels as its standard panelized system (Pioneer Bridges, a Division of Bailey Bridges, Inc., 2015). Following the expiration of the patent on the Bailey system, Mabey Johnson Ltd. and Thos Storey (Engineers) Ltd./Acrow Group companies made further advances in panelized bridging systems (SDR Engineering Consultants, Inc., 2005).

Mabey Johnson Ltd. began manufacturing Bailey panels in 1967 and made significant improvements upon panel design. Mabey Johnson Ltd. developed the Mabey Super Bailey which featured higher grade steel, changes to web members and weldments to improve shear and fatigue performance, new swaybraces and transom clamps, steel decking, and all components were galvanized. Mabey Johnson Ltd. replaced the Mabey Super Bailey in 1983 with the Mabey Compact Bridge System (also known as Compact 100) that included improvements in steel grade, channel sections for vertical and diagonal members, and high strength steel transoms. In 1986, Mabey Johnson Ltd. developed the Compact 200 (Figure 1B) which improved upon the Compact 100 by increasing the panel depth to 2.13 m (7 ft) and used thicker web channel sections. These changes led to an increase in strength of 80% compared to the Compact 100 and 110% compared to the Bailey panel. Mabey Johnson Ltd. also developed the Mabey Universal Bridge, featuring longer and deeper panels [4.50 m (14.75 ft) long by 2.35 m (7.75 ft) high], additional chord reinforcement, and shear panels (Joiner, 2001).

The Acrow Panel Bridge, produced by Thos Storey (Engineers) Ltd. in 1971, improved upon the original Bailey panel by utilizing higher grade steel, rectangular hollow sections, and moving the transom position, resulting in an increase in shear capacity by 25% and in bending capacity by 25%. The panels and their components were either painted or galvanized and various decking options (in both wood and steel) were developed. Further improvements were made in 1987 with the Acrow Panel 500 Series which utilized a stronger and variable length transom, different placement of the transom (the same as that used in the Mabey Compact Bridge System), as well as stiffer deck components (Joiner, 2001). To compete with the Compact 200 panel, the Acrow Panel 700 Series Bridge was developed which features deeper panels [2.29 m (7.5 ft), Figure 1C] (Joiner, 2001; Acrow Corporation of America, 2009).

While each of these systems has made significant improvements from the first Bailey panelized bridges, design challenges for all of these panelized systems in their conventional girder-type configurations include material efficiency, lateral bracing, and achieving longer spans.

PRECEDENT

Precedent exists for adapting panelized bridge systems to be oriented in vertical and diagonal configurations - carrying axial and flexural loads - for alternative applications such as bridges and buildings (Figure 4). These examples are prior relevant work which demonstrates the feasibility of orienting panelized systems to carry loads differently than originally designed. The Pratt truss, bowstring truss, and network tied arch presented in this paper implement similar orientations of panels to carry both axial and flexural loads. This prior precedent is reviewed here.

Bridge Piers

Bridge piers can be constructed from panelized systems. For example, during World War II, piers were built of Bailey panels to support greater deck clearance for conventional Bailey systems (Figure 4A). Only minimal additional parts were required. In the field, piers up to 21.3 m (70 ft) high were successfully constructed (Thierry, 1946).

Suspension Bridges

In much the same fashion, towers fabricated from panels can be built for a suspension bridge and the deck can also be comprised of panels (Figure 4B) (Thierry, 1946; Hempsall and Digby-Smith, 1952). While this suspension bridge adaptation is not as quick to erect as a conventional system, the Bailey suspension bridge can support 356 kN (80 k) loads over spans between 61.0 and 122 m (200 and 400 ft). This was the only suspension form capable of carrying vehicular loads during the World War II and was a great asset, particularly in mountainous regions (Thierry, 1946).

Movable Bridges

Panelized systems can be implemented as retractable, vetical lift, or bascule bridges (Figure 4C) (Thierry, 1946; Joiner, 2001). For a vertical lift, the deck (comprised of girder configuration panels) is lifted between two towers (also comprised of panels) (Hempsall and Digby-Smith, 1952). Recently, Acrow panels have been implemented in this fashion for the Quincy-Weymouth bridge over the Massachusetts Fore River. This bridge features two 64.0 m (210 ft) spans that provide a clearance of 65.5 m (215 ft) when lifted (Acrow Corporation of America, 2014). For bascule bridges, the deck is also comprised of girder configuration panels. Acrow panels have been utilized for 30.5 m (100 ft) span bascule bridges (Joiner, 2001).

Construction

Panelized systems have been utilized for a variety of construction practices, including form-work supports and concrete-placing runways (Figure 4D) (Hempsall and Digby-Smith, 1952). Bailey panels have been widely implemented as falsework for the construction of long-term bridges (Anon., 1958; Harris, 1952). They have also been utilized to support the shuttering of large reinforced concrete structures, such as dams (Anon., 1954; Hempsall and Digby-Smith, 1952). More recently, an Acrow Bridge was installed at "Ground Zero," following the events of September 11, 2001 as a ramp to aid in the removal of debris and eventual reconstruction (SDR Engineering Consultants, Inc., 2005). They have also served as shoring systems for up to 2400 kN (540 k) (Acrow Bridge, 2015).

Buildings

Bailey panels can and have been used to construct buildings with clear spans of up to 45.7 m (150 ft) (Anon., 1954; Hempsall and Digby-Smith, 1952). These buildings are constructed by connecting Bailey panels to form both the vertical walls and roof of the structure (Figure 4D) (Anon., 1954).

NEW FORMS USING STANDARD PANELS

Toward achieving higher material efficiency and longer spans [approximately 91.4 m (300 ft)], three new configurations for panelized bridge systems have been developed: 1) Pratt truss, 2) bowstring truss, and 3) network tied arch. Each form was assumed to be comprised of 3.05 m (10 ft) long panels, i.e., the length of the commercially available Bailey, Mabey Johnson, and Acrow systems (Figure 1). Developing these forms is a challenging task since members need to be composed of a discrete number of panels. First, simplified geometric and structural analyses were performed to select forms. These simplified analyses do not require knowledge of section properties, and therefore the results of this section are applicable to any 3.05 m (10 ft) long panelized system. For the Pratt and bowstring trusses, the maximum number of panels per member was restrained to 10 [i.e., 30.5 m (100 ft) long]. This was selected to limit the length of vertical members and therefore require that the span to depth ratio exceed 3. Typically span to depth ratios between 5 and 8 are economic for simply supported trusses (Kulicki and Reiner, 2011). This requirement therefore sets a lower bound on this ratio to limit the solution space toward more economic forms. An upper bound on span to depth results from the constraint that members be comprised of a discrete number of panels (e.g., for the Pratt truss, the vertical member must have a minimum length to satisfy the pythagorean triple). For the Pratt truss this is a span to depth ratio of 10 and for the bowstring truss this is 20.

Pratt Truss Bridge

The Pratt truss form was developed by evaluating combinations of a discrete number of panels for each global truss member (i.e., upper chord, lower chord, vertical, and diagonal members). The upper and lower chords were constrained to be horizontal. The possible combinations for each triangle of the truss are primitive pythagorean triples and multiplications thereof. Since the maximum number of panels per member was limited to 10, four combinations result: 3-4-5, 4-3-5, 6-8-10, and 8-6-10 (where identifiers are the number of panels horizontally-vertically-diagonally, Figure 5).

Each of these forms was then evaluated for structural performance. Structural performance can be measured in many ways. For new panelized forms developed in this research, global buckling is a design limitation that is mitigated by lateral bracing. Lateral bracing, however, is expensive and time-consuming to install. With the aim of minimizing the amount of lateral bracing required, a structural performance metric related to susceptibility of member buckling was selected. This metric is quantified as the maximum magnitude of the force (F) times the member length (L) squared for all compressive members to relate to the critical Euler buckling load. This metric was evaluated using a simplified approach: forces in each member were calculated under a uniform unit load [14.6 kN/m (1 k/ft) discretized as point loads at each upper chord joint] across the full length of the span and across just half of the span (i.e., to simulate uneven live loads) using the method of joints. This analysis assumes that forms are comprised of one dimensional truss members with identical section properties (i.e., the analysis does not include the detail of the individual components of a panel). This simplified approach enabled a quick method for evaluation. In Figure 6, the structural performance metric (FL^2) for the four forms is compared to the total length of members in the truss - an indication of its total weight or amount of material required in a panelized context. The highlighted form features the lowest FL^2 and the lowest total length of members showing a good balance between performance and low weight. This form is selected for further study in this paper.

Bowstring Truss Bridge

Forms for the bowstring truss (Figure 7) were developed where the diagonal (D), vertical (Y), and lower chord (N) members were restrained to be a discrete number of panels. The upper chord was assumed to span between lower chord ends (N_1). Every permutation of integer number (ranging from 1 to 10) of panels for members D, Y, and N in each bay that results in a span exceeding 91.4 m (300 ft) was determined to develop a solution set of forms (1,999 forms in total).

Similarly to the Pratt truss, each form was evaluated in terms of the structural performance metric (FL^2) and total length of members (Figure 8). To calculate the structural performance metric related to buckling susceptibility, the forms were evaluated under a uniform unit load [14.6 kN/m (1 k/ft) discretized as point loads at each upper chord joint] across the full length of the span and across just half of the span using the method of joints (the same approach as for the Pratt truss). In Figure 8 there are many forms along the Pareto-optimal set (i.e., solutions that are not overshadowed by other solutions). Again, the goal is to balance the need for lateral bracing (related to the structural performance metric FL^2) and the weight or amount of material. For very low FL^2 values, there is a family of solutions with different varying total length of members. A solution among this family with the lowest total length of members and the second lowest value for FL^2 is highlighted and investigated further.

Network Tied Arch Bridge

A network tied arch form was investigated since the arch can be very light as bending is distributed through the hanger system (Tveit, 1987) and the tie eliminates the need to resolve the arch's horizontal thrust in substructure. The arch (Figure 9) was designed to be polygonal, with each segment equal to one panel length. It is semi-circular to enable the relative angle between each panel to remain constant, thereby facilitating uniform connection design throughout the arch. A span to depth ratio of 5 is typical for arches. To enable the arch and the deck to be comprised of an even number of panels, the span to depth ratio is slightly lower: 4.39. Hanger cables should be inclined and intersect to minimize bending in the arch. Steep angles of cable inclination are more effective in carrying load, but can relax under asymmetric loads resulting in bending in the arch. Flat angles can cause higher bending in the arch (Tveit, 1987). To balances these effects and also facilitate hanger attachment to each panel (at panel middle) along the arch and the girder, hanger angles vary from 45.5 to 67.2 degrees.

Discussion

Three new forms have been developed through these simplified analyses, each offering different advantages and disadvantages. The Pratt truss form features repeated member joint angles, meaning that only a few member-to-member connection types would be needed throughout the form. This would result in savings in terms of design, manufacturing of the connection details, and erection. In comparison, the bowstring truss forms may have varying member connection angles, but less overall panels could be used. As shown in Figure 7, there are many bowstring solutions with less than 300 m (984 ft) of member lengths with comparable value for FL^2. The network tied arch offers an alternative option which features repeated connection angles and a means of distributing bending through its hanger system. Overall, these studies demonstrated a technique for rapidly evaluating panelized bridge forms and developed three forms for further study.

PARAMETRIC EVALUATION OF LATERAL BRACING STRATEGIES

For each of the forms considered in this paper, global buckling is a design limitation that must be mitigated by lateral bracing. To determine an effective strategy for lateral bracing, parametric studies were performed to evaluate the effect of (1) transverse spacing between panels and (2) stiffness of lateral struts connecting panels through moment-resisting connections [quantified by a multiplier of the moment of inertia of the panel chord which was taken as the base property for this member (I factor, hereafter)] on the behavior of panels aligned in girder-like and column-like configurations under horizontal and vertical loads (separately). These configurations were chosen to explore the efficacy of the bracing strategies in a bending-governed (i.e., where the lower chords are primarily in compression and the upper chords are primarily in tension for a cantilever scenario) and an axial load-governed environment (i.e., where all chords are in compression), respectively. Members in the new forms developed for this research would be subject to both bending and axial load, making an investigation of both loading environments necessary. Note that the girder-like configuration is oriented as a cantilever as opposed to a simply supported beam. If load were applied to nodes (i.e., locations where vertical or diagonal components meet the chords) in a simply supported beam environment with the same length, the dominant behavior would be shifted towards local buckling of the vertical or diagonal members in the panel. To focus instead on the global buckling behavior, a cantilever configuration was selected. These studies focused on (1) intra-plane strategies to connect closely spaced panel planes and (2) inter-plane strategies to connect planes of panels across the deck. A linear (eigenvalue) buckling analysis was performed in the software package SAP 2000 to evaluate the bracing strategies by solving the following problem:

$$[K_s - \lambda g(p)]\Psi = 0 \tag{1}$$

where K_s is the stiffness matrix, λ is the eigenvalue matrix, g is the geometric stiffness for loads p, and Ψ is the eigenvector matrix (Computers and Structures, Inc., 2015). This analysis is performed using the cross-sectional properties of the Bailey panel since it was the first panelized system developed. However, this analysis is focused on global buckling behavior and therefore the findings should be similar for any of the panelized systems. This selection does not indicate any preference by the authors for one system over another.

Note that the strategies investigated here could also enhance the performance of conventional configurations for panelized systems.

Intra-plane Bracing Strategies

To investigate intra-plane bracing strategies, three-dimensional finite element models of a 15.2 m (50 ft) long girder-like configuration (Figure 10A) and a 9.14 m (30 ft) tall column-like configuration (Figure 11A) featuring two planes of panels were built. The girder is a cantilever with pin-restraints (i.e., translation restrained in all directions) at four nodes. The column is pin-restrained at four nodes at the bottom. At the top four nodes, translation is restrained in the horizontal direction only. Vertical (emulating gravity loads) and horizontal (emulating wind loads) loads were applied separately to each, with a total magnitude of 4.45 kN (1 k). For the girder-like configuration, the total vertical load was applied via point loads on nodes [every 0.762 m (2.5 ft)] along the upper chord of each panel plane. For the column-like configuration, the total vertical load was applied via four point loads at the top of the column. For both configurations, the total horizontal load was applied via point loads on one plane of panels at nodes at each strut connection [every 3.05 m (10 ft)].

In a girder-like configuration (Figure 10) under vertical load, gains in the buckling factor (i.e., factor by which the load would need to be multiplied by to induce buckling) begin to asymptote as the spacing and I factor are increased at approximately a spacing of 0.914 m (3 ft) and an I factor of 2. Under horizontal loads, these gains are closer to linear. In a column-like configuration (Figure 11) under vertical load, the gains in the buckling factor begin to asymptote while more linear gains are observed under horizontal load. In both configurations, the panel spacing has a larger impact on performance under horizontal loads than the I factor, as expected. Under vertical loading, both the spacing and I factor are important parameters for design.

To achieve a strategy that is effective in girder-like and column-like configurations under horizontal and vertical loads, a spacing of 0.914 m (3 ft) and an I factor of 2 (i.e., two times the moment of inertia of the panel chord) was selected. This is approximately where the girder buckling factor under vertical loads asymptotes and close to where the column buckling factor under vertical loads also asymptotes. While higher spacing and higher I factors could further improve performance, this combination was selected as a balance between performance and the additional cost of stiffer and longer struts.

Inter-plane Bracing Strategies

To investigate inter-plane bracing strategies, three-dimensional finite element models in girder-like and column-like configurations that feature two sets of the intra-plane bracing systems connected by struts were built (Figure 12 and Figure 13). A spacing of 4.57 m (15 ft) for inter-plane bracing is used (and not varied) as this would be needed for one lane of vehicular traffic. The intra-plane bracing scheme selected from the previous section is used. This study varies the I factor for the inter-plane strut only. The boundary conditions for these studies are the same as that in the intra-plane studies. To make these studies comparable to the intra-plane studies, vertical and horizontal loads were applied separately, with a total magnitude of 8.90 kN (2 k), i.e., twice that of the intra-plane systems. The vertical loads were applied along the top chords of each plane of panels at the same nodes as the intra-plane study. The horizontal loads were applied along just one plane of panels at each strut connection.

In both girder-like and column-like configurations under vertical loads, the inter-plane strut I factor has limited effect on buckling behavior. The intra-plane configurations are effectively acting independently under this loading as the buckling factors are approximately the same as that from the intra-plane studies. The inter-plane bracing becomes activated under horizontal loads as expected.

Ultimately, an I factor for the inter-plane strut was selected to be the same as that for the intra-plane bracing: 2. This contributes to the overall focus on modular construction and minimizing the number of different parts.

ANALYSIS OF NEW FORMS

The previous sections developed new forms for bridges comprised of 3.05 m (10 ft) long panels and evaluated bracing strategies for panels. To show the promise of these forms, implementing also the selected bracing strategy, three-dimensional finite element analyses of the forms were performed. Like the parametric bracing study, these analyses use the Bailey panel. However, this research is focused on global buckling behavior and therefore the findings should be similar for any of the panelized systems.

Modeling Assumptions and Loading

These forms (Figure 14) are analyzed using three-dimensional finite element models in the software package SAP 2000 (Computers and Structures, Inc., 2015) under dead, distributed live load as per American Association of State and Highway Transportation Officials (AASHTO) Load and Resistance Factor Design Specification (AASHTO, 2012) [9.40 kN/m (0.64 k/ft), across the entire span and half of the span], and wind load [2.39 kPa (50 psf)]. A linear (eigenvalue) buckling analysis (as discussed in the previous section) was performed for each form.

Each form is comprised of four planes of panels. Individual panel components are welded together to form a complete, prefabricated panel. Therefore, moment-resisting connections between panel components are modeled. Experimental and numerical studies by King et al. (2013) indicate that this is a reasonable modeling assumption. Panel-to-panel connections are achieved by pins at the upper and lower chords. This transfers moment between panels and therefore panel-to-panel connections are modeled as moment-resisting. All components are A242 steel with a yield strength of 345 MPa (50 ksi) (Pioneer Bridges, a Division of Bailey Bridges, Inc., 2015). Panel planes are connected by the intra- and inter-plane bracing schemes determined in the previous section. Live load is applied to a single longitudinal member which is supported by inter-plane struts that carry the load to the panel planes.

Longitudinal and vertical boundary conditions (i.e., pin and roller restraints) are indicated in Figure 14. For the Pratt and bowstring trusses, a longitudinal pin restraint is applied to just one plane of panels on one end; the rest of the longitudinal restraints are rollers (i.e., translation restrained in the vertical direction). For the network tied arch, all planes are restrained by longitudinal pins at both ends. In reality, the tie would carry the horizontal reaction from the arch. The design of the tie would occur in a final detailed design stage and so it is not modeled here for simplicity. For all forms, translation in the transverse direction is restrained at the end of each plane of panels.

Pratt Truss Bridge

With a geometry of the Pratt truss determined (Figure 6), a three-dimensional finite element model was built (Figure 14A) and analyzed as discussed above. Each truss plane is comprised of 117 panels, meaning a total of 468 panels are needed to carry one lane of vehicular traffic. The upper and lower chord are braced by the intra- and inter-plane bracing schemes selected. Intra-plane bracing is implemented in the verticals and diagonals, but no inter-plane bracing is required for these members. With these bracing strategies, the system buckles in the upper chord in localized regions toward the center of span (Figure 15A) with a buckling factor of 4.09 under dead, live (dominant buckling mode corresponds to case when live load applied across entire span), and wind loads.

Bowstring Truss Bridge

Using the form of the bowstring truss highlighted in Figure 8, a finite element model of this form was built (Figure 14B) and analyzed. Each truss plane is comprised of 124 panels (a total of 496 for the span). Like the Pratt truss, the upper and lower chords are braced by the intra- and inter-plane bracing, with the verticals and diagonals requiring only intra-plane bracing. Under dead, live (dominant buckling mode corresponds to case when live load applied across entire span), and wind loads, the dominant buckling mode of the system (Figure 15B) is global with a factor of 6.03.

Network Tied Arch Bridge

A finite element model of the network arch from (Figure 14C) was analyzed. The arch includes four planes of panels (34 panels each) connected by the intra- and inter-plane bracing strategies. The girder is just two planes connected by inter-plane bracing. A total of 196 panels would be needed for the entire span (including the girder). The global buckling analysis showed the stability of the form. The critical buckling factor under dead, live (dominant buckling mode corresponds to case when live load applied across entire span), and wind loads is 2.48 with a global buckling mode observed (Figure 15C).

Discussion

These preliminary finite element analyses have shown the promise of each form and the developed bracing strategy. These forms can be compared to the conventional girder configuration which requires 378 panels to span 64.0 m (210 ft) using the Bailey panelized system. The Pratt truss [468 panels for a 96.0 m (315 ft) span], the bowstring truss [496 panels for a 104 m (340 ft) span], and the network tied arch [196 panels for 91.4 m (300 ft) span] can achieve longer spans. To compare these forms, a material efficiency metric is defined as the span length squared divided by the number of panels. The numerator of this metric is selected since the moment demand for a simply supported beam in a uniformly loaded environment would be proportional to the span squared. The efficiency metric for the conventional bailey system is 117, for the Pratt truss is 212, for the bowstring truss is 233, and for the network tied arch is 459. In summary, all three new forms show significantly higher efficiency than the conventional system, with the network tied arch far exceeding the rest.

This study focused on analyzed forms with an approximately 91.4 m (300 ft) span carrying one vehicular lane of traffic. Longer spans and/or higher loads could be achieved by further improving the lateral bracing strategy or by increasing the strength of the panels. For example, if the I factor for the intra- and inter-plane struts of the bowstring truss form is increased from 2 to 5, the buckling factor increases by a factor of 1.47. If the intra-plane spacing is increased from 0.914 m (3 ft) to 1.52 (5 ft), the buckling factor increases by a factor of 1.39. Future areas for research include also investigating the impact of stronger panels on system behavior.

This analysis has focused on global behavior of the system through a linear (eigenvalue) buckling analysis. To further develop these forms and the bracing strategy for field implementation, nonlinear buckling analyses (incorporating geometric nonlinearities) should be considered to account for manufacturing imperfections and deformations induced by lateral loads. The strength of individual components would need to be evaluated under factored loads as per AASHTO specifications (including also the moving design vehicle point loads). Detailed connection design, both panel-to-panel along a member and at member junctures, would be required. Substructure design would also be necessary. Cyclical loading and fatigue life would also be a critical area for future investigation.

OPTIMIZATION OF PANEL LENGTH

The first part of this paper has focused on new bridge forms comprised of standard, commercially available 3.05 m (10 ft) long panels. However, more forms could be developed if the solution space is widened beyond this standard length panel using structural optimization. An optimization procedure is developed and demonstrated for the bowstring truss form.

Optimization Problem

To determine optimized panel lengths and forms, a multi-objective optimization procedure has been implemented for minimum self-weight (W, quantified as the total length of panels and calculated as the length of the panel, l_{panel}, times the total number of panels, N) and maximum structural performance (A, i.e., minimizing the structural performance metric related to buckling resistance, quantified as the maximum value of FL^2, where F is the force in the member and L is the member length, for all N_c number of compression members in the form) as defined in the following problem formulation:

$$\begin{aligned} \underset{\mathbf{z}}{\text{minimize}} \quad & W(\mathbf{z}) = l_{panel}(\mathbf{z})N(\mathbf{z}) \\ & A(\mathbf{z}) = \max(\{F_i(\mathbf{z})L_i(\mathbf{z})^2 : i = 1, ..., N_c(\mathbf{z})\}) \\ \text{such that} \quad & c(\mathbf{z}) \leq 0 \end{aligned} \tag{2}$$

where **z** is a design variable that defines the form, including the panel length, the total number of panels, and the geometric coordinates of the form. This design variable is selected from a database that includes every permutation of form for a bowstring truss with a span exceeding 91.4 m (300 ft) with panel lengths ranging from 1.52 m to 6.20 m (5 ft to 20ft) in increments of 0.305 m (1 ft). Constraints (c) have been implemented in the generation of this database so that only feasible forms are considered. For the the bowstring truss form, this means that the diagonal, vertical, and lower chord members were constrained to be a discrete number of panels. Each member is also constrained to be less than 30.5 m (100 ft) as considered in the previous studies. Note that duplicate forms result in which the same form can be comprised of different panel lengths [e.g., a form using a 3.05 m (10 ft) panel length could also be comprised of 1.52 m (5 ft) panels using twice the number of panels]. In these cases, the database entries using the shorter panel length were eliminated in favor of the form with the longer panel length (as reducing number of panel-to-panel connections would improve the design). These constraints resulted in a database of 523,136 possible forms. The database was ordered by increasing span to depth ratio. The force in members is determined using the method of joints as discussed earlier in the paper under a uniformly distributed unit load across the full span and across half of the span.

It is important to note in the development of this optimization procedure that minimum self-weight does not necessarily indicate lowest cost since this metric does not include fabrication or field labor costs. In this context, fabrication costs will relate to the design of individual panels which is not considered in this study. Field labor costs relates to the number of global joints of the structure (i.e., number of member-to-member connections) which is evaluated in the results sub-section. Minimum self-weight is simply used as one metric of efficiency.

Optimization Algorithm

The heuristic search algorithm Simulated Annealing (SA) was implemented for this optimization problem since it is a fast and effective iterative improvement algorithm which has been implemented for a broad range of structural optimization problems [e.g., Shea and Smith (2006); Paya et al. (2008); Ohsaki et al. (2009)], including modular [e.g., Alegria Mira et al. (2015); Quaglia et al. (2014); Martinez-Martin and Thrall (2014); Russell et al. (2014)] or deploying structures [e.g., Thrall et al. (2014, 2012)].

The SA algorithm, based on the process of controlled cooling of metals, begins by selecting an initial random solution (in this research, a form from the database discussed above). A new solution is then found by randomly perturbing the initial selection [i.e., moving up or down the database of forms by a random magnitude]. If the value of the objective function for this new solution is less than that of the first solution, it becomes the current solution for further iteration. If not, a probability of keeping this second solution as the current solution is calculated: $P = e^{-\Delta F/T}$, where F is the value of the objective function and T is the temperature [a parameter that is initially chosen to select between 20 and 40 percent of higher value solutions (Medina, 2001)]. This probability of continuing to iterate upon higher value solutions enables the algorithm to avoid local minima. This iteration continues for a user-defined number of iterations called a cooling cycle. After each cooling cycle, the temperature is reduced by a user-defined number. The algorithm continues until there has been a user-defined number of cooling cycles in which there has been no improvement in the solution (Kirkpatrick et al., 1983).

A multi-objective version of this algorithm (MOSA) was used in this research. In this case, the algorithm iterates as mentioned above. However, new solutions are compared against a Pareto-optimal set of solutions. If the new solution is Pareto-optimal, it becomes the current solution. If it is not, there is a probability that the algorithm will continue to iterate on this solution, calculated by:

$$P = \prod_{i=1}^{Q} e^{-[F_i(z_1)-F_i(z_2)]/T_i}, \tag{3}$$

Here, Q is the total number of objective functions (in this case 2), F_i is the value of an objective function, z_1 is the current solution, and z_2 is the new solution. To explore the solution space fully, the algorithm uses an intelligent return-to-base strategy which selects a different Pareto-optimal solution upon which to iterate at the end of each cooling cycle. This strategy initially selects from any of the A_s number of Pareto-optimal solutions, but increasingly explores the more isolated (or extreme edges) of the Pareto-optimal set. Isolation of a solution is calculated as follows:

$$I(z_j) = \sum_{\substack{k=1 \\ k\neq j}}^{A_s} \sum_{i=1}^{Q} \left\{ \frac{F_1(z_k) - F_i(z_j)}{F_{imax} - F_{imin}} \right\}^2, \tag{4}$$

where F_{max} and F_{min} are the maximum and minimum values of each objective function, respectively, across the Pareto-optimal set. The solutions are ordered by amount of isolation and the algorithms selects from a smaller number of the more isolated solutions as it progresses (the number of solutions selected from is reduced by a factor of 0.9 at each cooling cycle). The algorithm continues to iterate until there have been the user-defined number of cooling cycles in which no new Pareto-optimal solutions were found (Suppapitnarm et al., 2000). With a final set of Pareto-optimal solutions at convergence, an engineer can choose an optimized solution.

Optimization Results and Discussion

Figure 16 shows the Pareto-optimal set developed through multi-objective optimization. The entire database was exhaustively evaluated to determine the global minimum for each objective function which are indicated by square markers. In addition to showing the values of each objective function, the plot indicates the length of the panel by the marker size and the number of global joints of the structure by the color.

As expected the global minimum for the sum of the member lengths objective function is a very shallow truss, while the global minimum for the structural performance metric (FL^2) is a very deep truss. Both found the smallest panel length: 1.52 m (5 ft). This is also expected as the smaller panel lengths provide more flexibility in the global form.

The Pareto-optimal set spans between these extremes. Several highlighted forms show that as the sum of the member lengths increases and the susceptibility to buckling decreases (i.e., along the curve from right to left), the truss form evolves from a shallow triangle to a deeper truss with a curved lower chord. The number of global joints also increases as expected. Most forms have the smallest panel length [1.52 m (5 ft)], while a few have longer (indicated by larger marker sizes). There is a family of solutions at the knee of the Pareto-optimal curve which feature low values for both objective functions with also a low number of global joints. This family would be particularly appealing from a design and constructability perspective. More specifically, a low number of global joints would reduce cost and construction complexity. As noted earlier, these factors were not explicitly included in the optimization procedure. Examining this family of solutions, which already achieves low values for the objective functions, facilitates incorporating these factors into design.

CONCLUSION

This paper addressed three design challenges for panelized bridge systems: (1) efficient use of material, (2) lateral bracing, and (3) achieving longer spans.

Toward achieving material efficiency and longer spans, this paper developed forms for a Pratt truss, a bowstring truss, and a network tied arch (Figure 14) with spans exceeding 91.4 m (300 ft). Each is comprised of standard 3.05 m (10 ft) long panels (i.e., the length of each of the panels in the Bailey, Mabey Johnson and Acrow systems, Figure 1). The promise of these forms was demonstrated through linear (eigenvalue) buckling analyses of these forms under dead, live, and wind loads. A material efficiency metric was used to compare each of these forms to one another and to a conventional configuration. Each new form was shown to be more efficient, with the network tied arch far out-performing the rest. The network tied arch also features some construction advantages. This includes repeated connection angles, meaning that only one member-to-member connection type is needed for the entire system. With these advantages and the enhanced material efficiency, the network tied arch can be considered the most promising form.

To also develop an effective lateral bracing strategy, parametric studies were performed on girder-like and a column-like configurations of panels which investigate the effect of spacing between planes of panels and bracing members on buckling behavior. An effective bracing strategy was developed based on these parametric studies and implemented for the three-dimensional analyses discussed above. With further research, the lateral bracing strategies developed in this paper could also be implemented for conventional configurations of panelized bridge systems.

Toward the field implementation of these new bridge forms, future areas of research include detailed final analysis and design. These analyses should include analysis and design under strength, extreme event, service, and fatigue limit states as prescribed per AASHTO. As noted earlier, nonlinear buckling analyses (incorporating geometric nonlinearities) should be considered. Further investigation of the modeling assumptions implemented here should be performed, including the panel-to-panel connections. Substructure design would also need to be performed.

To open the solution space beyond standard panelized systems, an optimization procedure was developed to determine an optimized panel length and form for panelized bridge systems. This optimization procedure was demonstrated for the bowstring truss form showing that a lower self-weight and a lower susceptibility to buckling can be achieved by moving away from the standard length panel. This opens a new opportunity for research in developing new panelized systems toward further improvements.

ACKNOWLEDGMENTS

This material is based upon work supported by the National Science Foundation under Grant No. CMMI-1351272. No funding was provided by any panelized bridge manufacturers. There is no conflict of interest in this research. The authors would like to thank Skip Wilson of Pioneer Bridges, a Division of Bailey Bridges, Inc. for providing cross-sectional properties for Bailey panels.

REFERENCES

AASHTO (2012). *AASHTO LRFD bridge design specifications, customary U.S. units*. American Association of State Highway and Transportation Officials, Washington, D.C.

Acrow Bridge (2015). “Acrow bridge. <http://www.acrow.com/> (May 26, 2015).

Acrow Corporation of America (2009). “Acrow 700XS panel bridge technical handbook. Acrow Corporation, Parsippany, NJ, 1-67.

Acrow Corporation of America (2014). “Quincy-Weymouth, Massachusetts Fore River Bridge. <http://acrow.com/wp-content/uploads/2013/05/Fore-River-Quincy-MA.pdf> (August 8, 2014).

Alegria Mira, L., Thrall, A. P., and De Temmerman, N. (2015). “The universal scissor component: Optimization of a reconfigurable component for deployable scissor structures.” *Engineering Optimization* In press.

Anon. (1954). “Bailey bridging in peacetime.” *Engineering*, 178(4620), 218–220.

Anon. (1958). “Bailey bridge units are versatile tool.” *Better Roads*, 28(5), 27–28.

Computers and Structures, Inc. (2015). “Sap 2000: Integrated software for structural analysis and design. <http://www.csiamerica.com/products/sap2000> (February 5, 2015).

Department of the Army (1986). “Bailey bridge.” *Field Manual No. 5-277*, Headquaters, Department of the Army, Washington, DC.

Harris, R. C. (1952). “Bailey bridge used as falsework for erection of bridge in B.C..” *Roads and Engineering Construction*, 90(10), 107, 148–150.

Hempsall, E. and Digby-Smith, R. (1952). “Bailey bridging of wartime fame has versatile civilian uses.” *Roads and Engineering Construction*, 90(7), 85–89,100.

Joiner, J. H. (2001). *One More River to Cross: The Story of British Military Bridging*. Pen and Sword Books Ltd, South Yorkshire, UK.

King, W. S., Wu, S. M., and Duan, L. (2013). "Laboratory load tests and analysis of bailey bridge segments." *Journal of Bridge Engineering*, 18(10), 957–968.

Kirkpatrick, S., Gelatt, C. D., and Vecchi, M. P. (1983). "Optimization by simulated annealing." *Science*, 220(4598), 671–680.

Kulicki, J. M. and Reiner, B. M. (2011). "Truss bridges." *Structural Steel Designer's Handbook*, R. Brockenbrough and F. Merritt, eds., McGraw Hill, New York.

Mabey (2015). "Temporary and permanent bridges. <http://www.mabey.com/products-services/permanent-temporary-bridge/> (May 26, 2015).

Martinez-Martin, F. J. and Thrall, A. P. (2014). "Honeycomb core sandwich panels for origami-inspired deployable shelters: Multi-objective optimization for minimum weight and maximum energy efficiency." *Engineering Structures*, 69, 158 – 167.

Medina, J. R. (2001). "Estimation of incident and reflected waves using simulated annealing." *Journal of Waterway, Port, Coastal, and Ocean Engineering*, 127(4), 213–221.

Ohsaki, M., Tagawa, H., and Pan, P. (2009). "Shape optimization of reduced beam section under cyclic loads." *Journal of Constructional Steel Research*, 65(7), 1511–1519.

Paya, I., Yepes, V., Gonzalez-Vidosa, F., and Hospitaler, A. (2008). "Multi-objective optimization of concrete frames by simulated annealing." *Computer-Aided Civil and Infrastructure Engineering*, 23(8), 596–610.

Pioneer Bridges, a Division of Bailey Bridges, Inc. (2015). "Bailey bridges. <http://www.baileybridge.com/> (February 6, 2015).

Quaglia, C. P., Yu, N., Thrall, A. P., and Paolucci, S. (2014). "Balancing energy efficiency and structural performance through multi-objective shape optimization: Casey study of a rapidly deployable origami-inspred shelter." *Energy and Buildings*, 82, 733–745.

Russell, B. R. and Thrall, A. P. (2013). "Portable and rapidly deployable bridges: Historical perspective and recent technology developments." *Journal of Bridge Engineering*, 18(10), 1074–1085.

Russell, B. R., Thrall, A. P., Padula, J. A., and Fowler, J. E. (2014). "Reconceptualization and optimization of a rapidly deployable floating causeway." *Journal of Bridge Engineering*, 19(4), 04013013.

SDR Engineering Consultants, Inc. (2005). "Prefabricated steel bridge systems: Federal Highway Administration (FHWA) solicitation no. DTFH61-03-R-00113 (September). FHWA, <www.fhwa.dot.gov/bridge/prefab/psbsreport.pdf> (April 6, 2012).

Shea, K. and Smith, I. F. C. (2006). "Improving full-scale transmission tower design through topology and shape optimization." *Journal of Structural Engineering*, 132(5), 781–790.

Suppapitnarm, A., Seffen, K. A., Parks, G. T., and Clarkson, P. J. (2000). "Simulated annealing algorithm for multi-objective optimization." *Engineering Optimization*, 33(1), 59–85.

Thierry, J. A. (1946). "The Bailey bridge." *The Military Engineer*, 38(245), 96–102.

Thrall, A. P., Adriaenssens, S., Paya-Zaforteza, I., and Zoli, T. P. (2012). "Linkage-based movable bridges: Design methodology and three novel forms." *Engineering Structures*, 37, 214–223.

Thrall, A. P., Zhu, M., Guest, J. K., Paya-Zaforteza, I., and Adriaenssens, S. (2014). "Structural optimization of deploying structures composed of linkages." *Journal of Computing in Civil Engineering*, 28(3), 04014010.

Tveit, P. (1987). "Considerations for design of network arches." *Journal of Structural Engineering*, 113(10), 2189–2207.

List of Figures

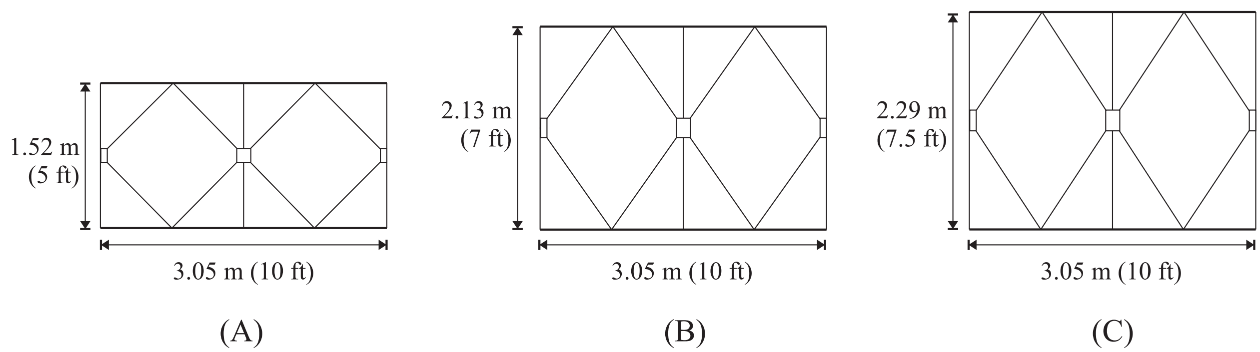

FIG. 1. Elevation views of (A) Bailey [Standard US Army M2 (Pioneer Bridges, a Division of Bailey Bridges, Inc., 2015)], (B) Mabey Johnson [Compact 200 (Mabey, 2015)], and (C) Acrow [700XS, (Acrow Corporation of America, 2009)] panels.

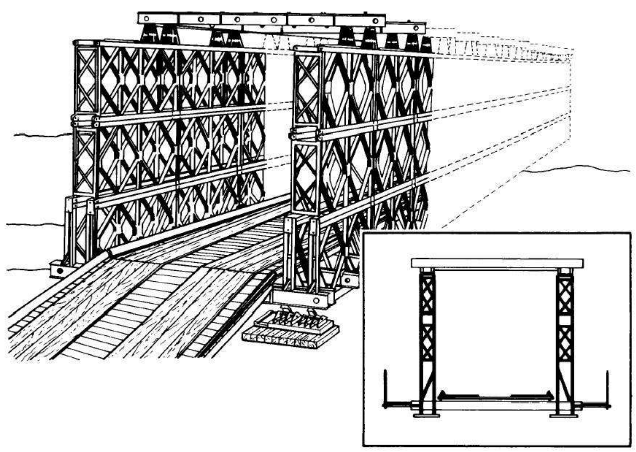

FIG. 2. Double-triple configuration of Bailey Bridge panels, including isometric and section views. Images courtesy of US Army (Department of the Army, 1986).

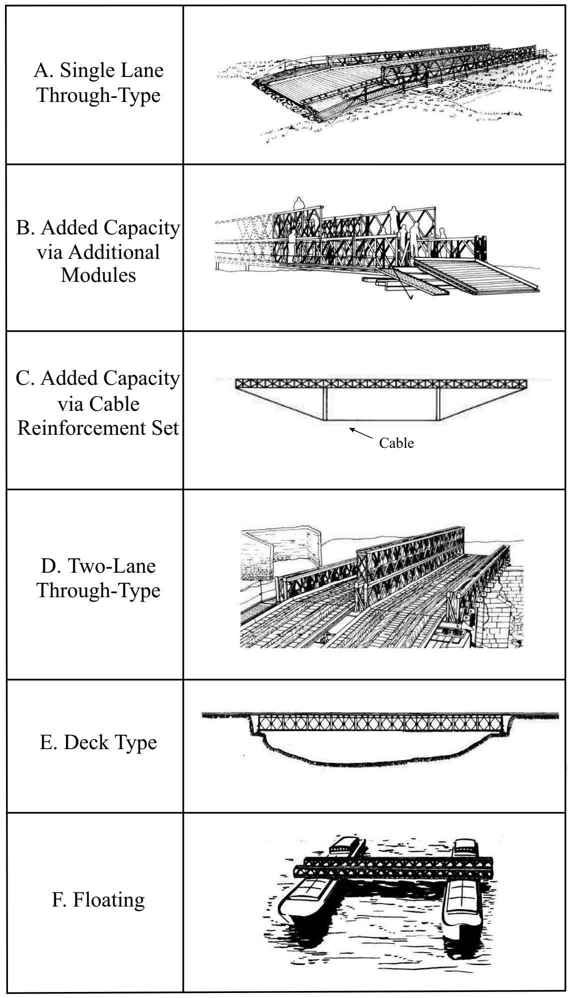

FIG. 3. Conventional implementations of Bailey Bridge system, including (A) single-lane through-type, (B) with additional panels for added capacity, (C) with a cable reinforcement set for added capacity, (D) two-lane through-type, (E) two-lane deck type, and (F) floating. Images courtesy of the US Army (Department of the Army, 1986)

A. Piers	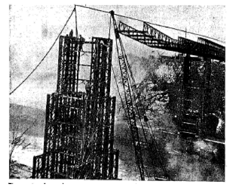
B. Suspension Bridges	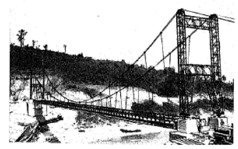
C. Moveable Bridges	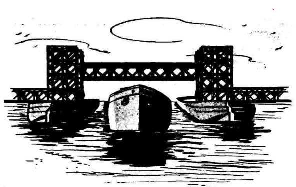
D. Runways	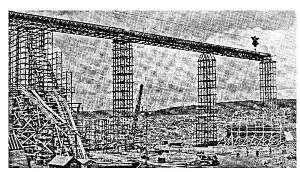
E. Buildings	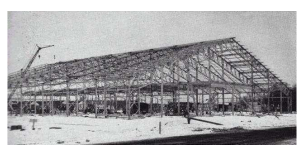

FIG. 4. Precedent for alternative implementations of panelized bridge systems, including (A) piers (Thierry, 1946), with permission from the Society of American Military Engineers, (B) suspension bridges (Thierry, 1946), with permission from the Society of American Military Engineers, (C) moveable bridges, image courtesy of US Army (Department of the Army, 1986), (D) runways (Hempsall and Digby-Smith, 1952), with permission from Roads & Bridges, and (E) buildings (Hempsall and Digby-Smith, 1952), with permission from Roads & Bridges.

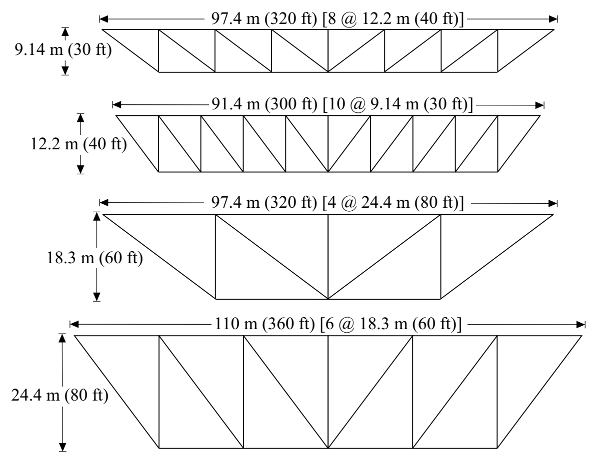

FIG. 5. Elevation views of the four combinations of Pratt trusses evaluated.

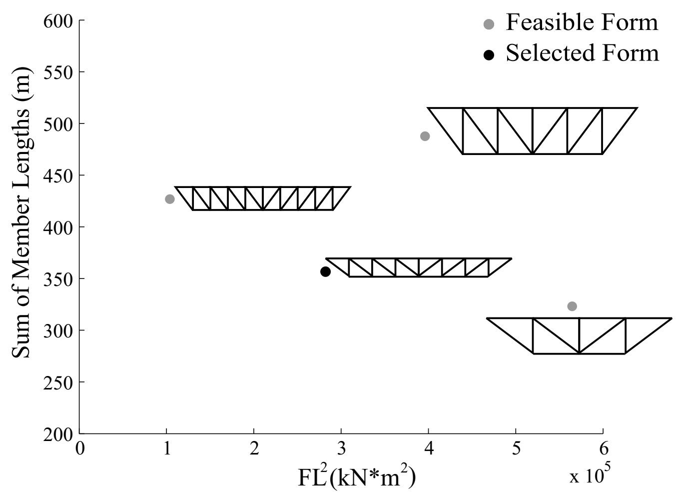

FIG. 6. Selection of Pratt truss form: Comparison of total length of panels to structural performance metric (FL^2). All feasible forms are sketched.

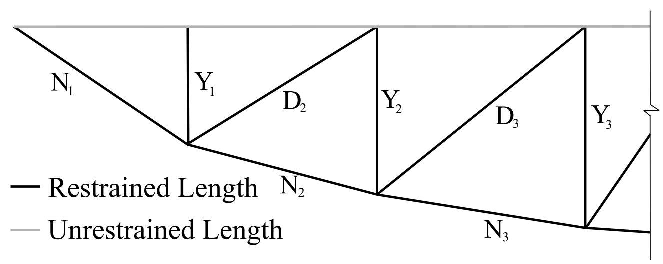

FIG. 7. Partial elevation view of bowstring truss form.

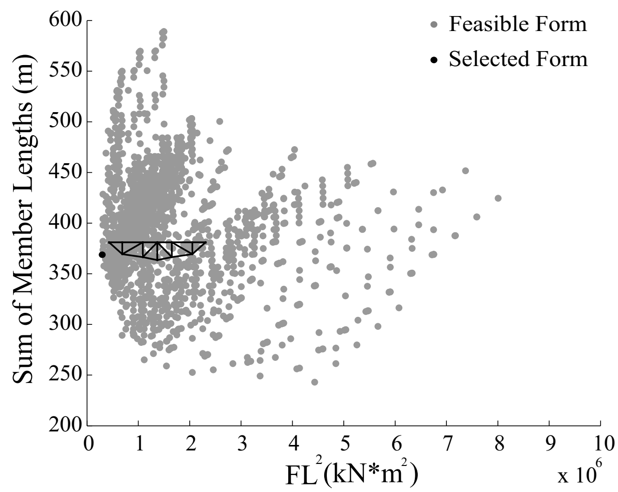

FIG. 8. Selection of bowstring truss form: Comparison of total length of panels to structural performance metric (FL^2). The selected form is sketched.

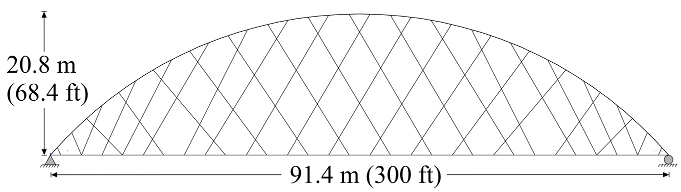

FIG. 9. Elevation of network tied arch form.

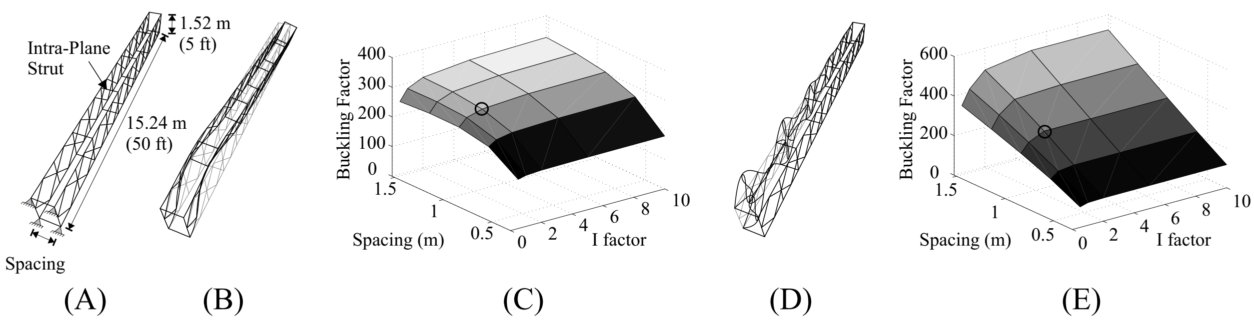

FIG. 10. Parametric study of intra-plane bracing in a girder-like configuration, including (A) isometric view indicating dimensions and boundary conditions, (B) buckled shape under vertical load (for selected option), (C) buckling factor under vertical load as a function of spacing and I factor (selected option is highlighted) (D) buckled shape under horizontal load (for selected option), and (E) buckling factor under horizontal load as a function of spacing and I factor (selected option is highlighted).

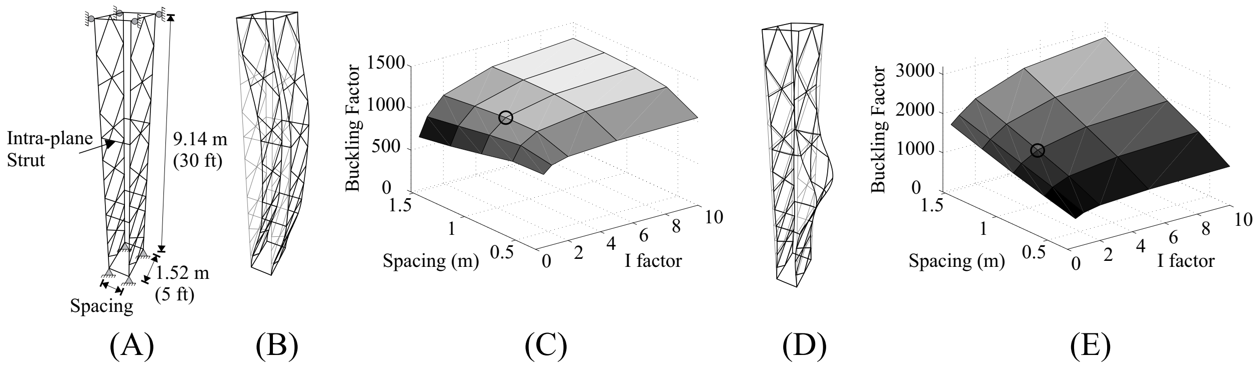

FIG. 11. Parametric study of intra-plane bracing in a column-like configuration, including (A) isometric view indicating dimensions and boundary conditions, (B) buckled shape under vertical load (for selected option), (C) buckling factor under vertical load as a function of spacing and I factor (selected option is highlighted) (D) buckled shape under horizontal load (for selected option), and (E) buckling factor under horizontal load as a function of spacing and I factor (selected option is highlighted).

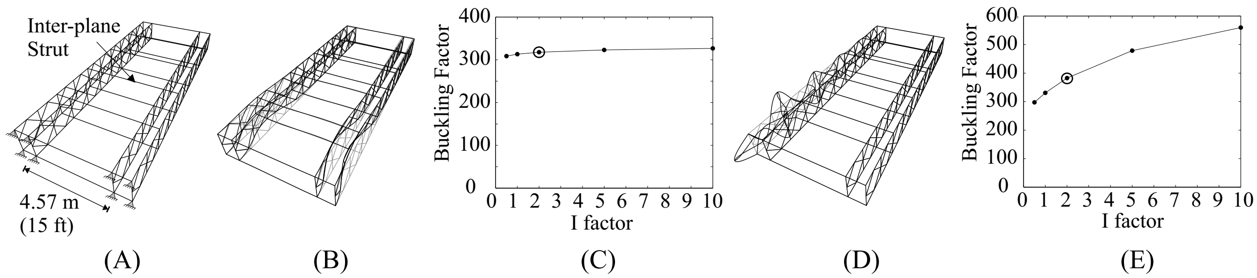

FIG. 12. Parametric study of inter-plane bracing in a girder-like configuration, including (A) isometric view indicating boundary conditions, (B) buckled shape under vertical load (for selected option), (C) buckling factor under vertical load as a function of I factor (selected option is highlighted) (D) buckled shape under horizontal load (for selected option), and (E) buckling factor under horizontal load as a function of I factor (selected option is highlighted).

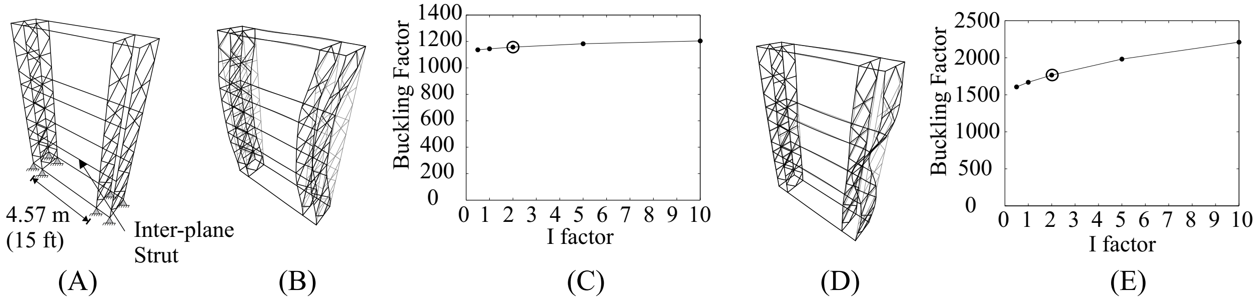

FIG. 13. Parametric study of inter-plane bracing in a column-like configuration, including (A) isometric view indicating boundary conditions, (B) buckled shape under vertical load (for selected option), (C) buckling factor under vertical load as a function of I factor (selected option is highlighted) (D) buckled shape under horizontal load (for selected option), and (E) buckling factor under horizontal load as a function of I factor (selected option is highlighted).

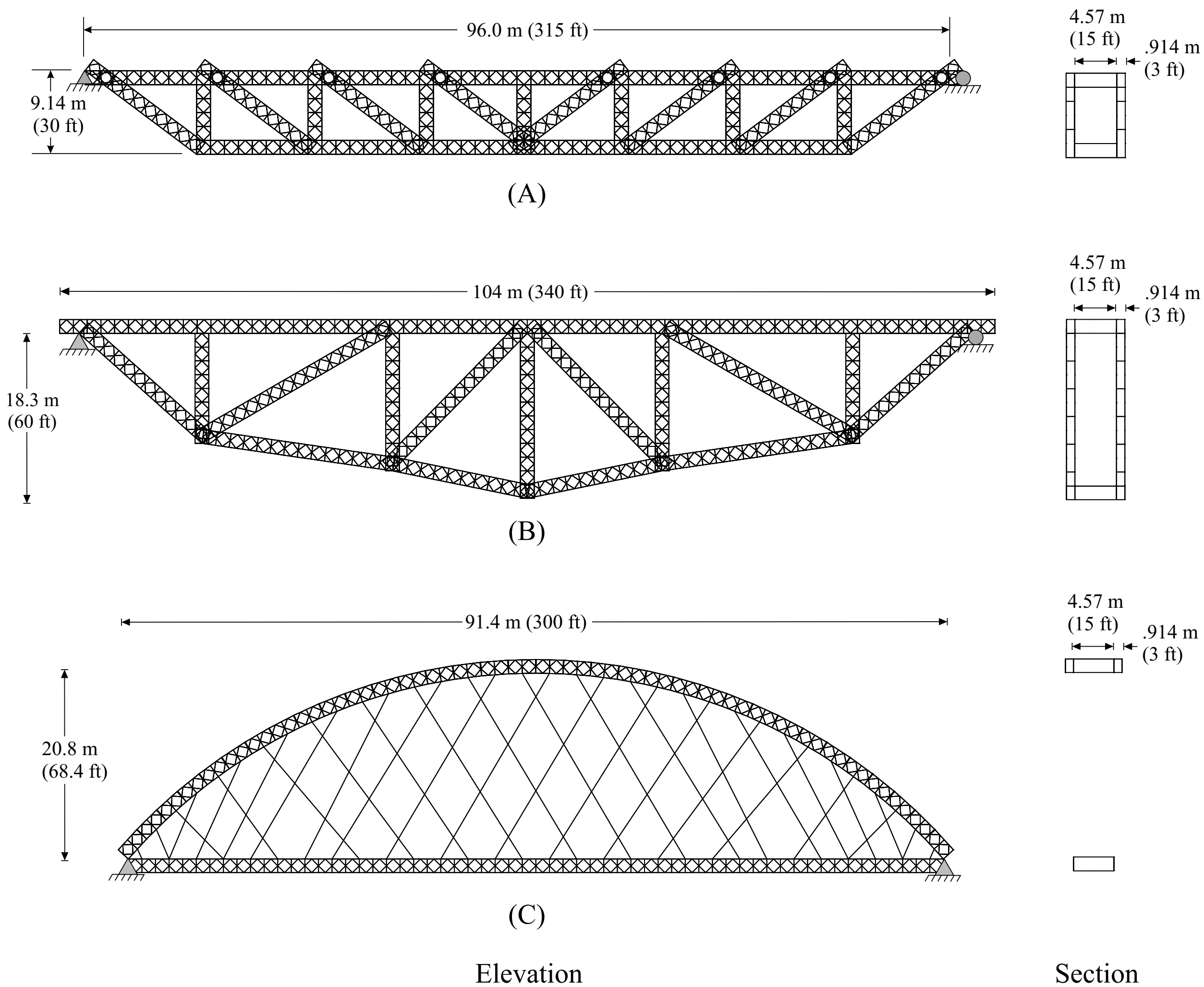

FIG. 14. New bridge forms in elevation view (left) and section view (right): (A) Pratt truss, (B) bowstring truss, and (C) network tied arch.

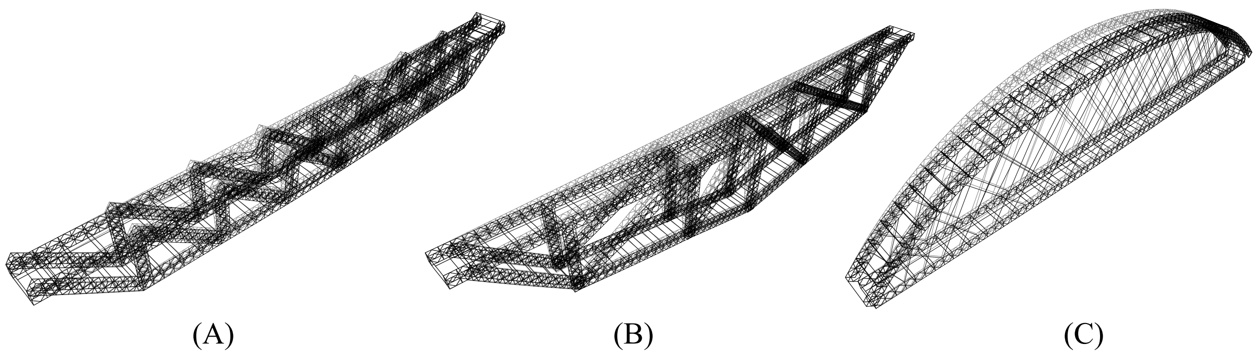

FIG. 15. Buckled shapes of the new bridge forms: (A) Pratt truss, (B) bowstring truss, and (C) network tied arch.

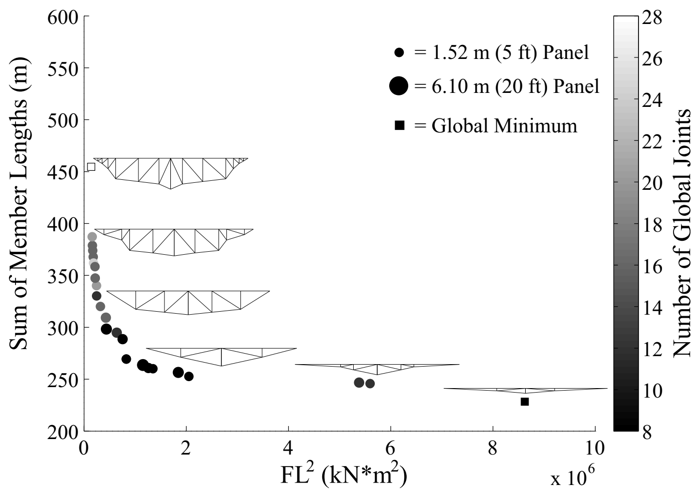

FIG. 16. Results of multi-objective optimization procedure for the bowstring truss form. Marker size indicates the number of panels and grayscale coloring indicates the number of global nodes. Global minima included for reference.